

CREEP RATE SPECTROSCOPY: HIGH-RESOLUTION ANALYSIS OF RELAXATIONS AND PREDICTION OF ANOMALIES IN MECHANICAL BEHAVIOR OF SOLIDS

Vladimir A. Bershtein*, Pavel N. Yakushev, Nina N. Peschanskaya

Ioffe Physico-Technical Institute, Russian Academy of Sciences,
194021 St.Petersburg, Russia

SUMMARY: An original laser-interferometric creep rate spectroscopy method was applied to analysis of molecular motion in some polymers, composites and interpenetrating polymer networks. Its potentials for study of nanoscale dynamic/compositional heterogeneity in complex systems, of a peculiar relaxation behavior of polymer binder in composites, and for prediction of temperature anomalies in strength are demonstrated.

INTRODUCTION

The creep rate spectroscopy (CRS) technique, developed in our laboratory, was previously applied to research of precise deformation kinetics (Refs. 1-3), and discrete analysis of molecular motion in polymers (Refs. 3-5) including networks and interpenetrating networks (IPN) (Refs. 6,7). This method exhibited obvious superiority in resolution to the generally used relaxation spectrometry techniques and allowed to study in detail relaxations much below, near, and above glass transition temperature, to trace fine changes in relaxation characteristics as well as to reveal and analyze relaxations in brittle materials (Refs. 8,9) where other approaches to this problem are difficult to realize. This paper reports on CRS data manifesting (a) correlation of a creep rate (CR) spectrum with the fracture - temperature dependence, (b) special relaxation behavior of a polymer binder in composite, and (c) dynamic heterogeneity within a broad IPN glass transition.

EXPERIMENTAL

Two CRS setups, operating under an uniaxial compression or extension, were used; their schemes were described elsewhere (Refs. 3,5). A Michelson interferometer utilizing the He-Ne laser was used for optical recording the creep rates. The time evolution of the creep process under small stresses was recorded as an interferogram obtained due to the Doppler effect. The beat frequency ν yielded a creep rate $\dot{\epsilon}$ by a formula:

$$\dot{\epsilon} = \frac{\lambda \nu}{2l_0} \quad (1)$$

where $\lambda = 630$ nm is a laser wavelength, and l_0 is an initial length of a sample.

High sensitivity of this technique allowed measuring the creep rates $\dot{\epsilon} \approx (10^{-8}-10^{-3}) \text{ s}^{-1}$ at low stresses, much lower than the yield stress, on the basis of creep deformation of ca. 0.01 % at $T < T_g$ or a few percent within the glass transition. The instrumental accuracy of the $\dot{\epsilon}$ estimation did not exceed 1 %.

Under these conditions, creep was predominantly associated with local shear strains ('microplasticity'), and its rate decreased as the creep process proceeded. Therefore, besides a stress value, the time t from a moment of loading to onset of the measurement, as the second experimental parameter, was kept constant in measurements of the creep rates at different temperatures. Thus, time $t = 10$ or 30 s was chosen as optimum in these experiments. The correlative (equivalent) frequency of the experiments was equal to $\nu_{\text{corr}} = (2\pi t)^{-1} \approx 10^{-2} \text{ Hz}$.

The $\dot{\epsilon}$ vs. T dependences, creep rate spectra, were measured as follows. Cylinders 3 mm in diameter and 6 mm in height were used in the compression tests whereas the trowel-like film samples with the cross-section of the working part of $1 \times 5 \text{ mm}$ and $1 \times 10 \text{ mm}$ at the sample ends were taken for extension tests. The sample was cooled down to the lowest temperature of the temperature range under study and a small stress was applied for 1 min. After recording an interferogram, a sample was unloaded, heated at the rate of 1 K min^{-1} to a temperature 5 K higher and then was loaded again with the same stress; again, the interferogram was recorded, the sample was unloaded and so on. Under tension, a sample was set in special clamps providing high friction.

In these experiments, the creep rates were measured over the range 120 - 360 K. Significantly, because of a small deformation of the sample, its isostructural state is maintained during the measuring process. This was corroborated especially by a total recovery of an initial creep rate after unloading and a reverse temperature jump.

As a result, multiple peaks of increased creep rates may appear on the $\dot{\epsilon}$ vs. T curves measured in the way described (Refs. 3-7). Figure 1 shows a typical creep rate spectrum obtained in the region of the sub- T_g relaxations for a rather complex network, and the degree of spectral reproducibility for two samples taken from two separate batches. Some scattering in the peak height or temperature values is apparent. Nevertheless, complex structure of the spectrum and relative contributions of constituent peaks to the spectral contour are satisfactorily reproduced.

RESULTS AND DISCUSSION

Creep rate spectra and temperature anomalies in mechanical strength

Nonmonotonic changes in mechanical properties of polymers at certain characteristic temperatures were observed previously and associated with some kinds of molecular motion

(Refs. 11,12). The creep rate spectra are able to respond in a discrete manner to the 'unfreezing' of the multiple nanoscale segmental motions; therefore, correlations between the spectrum and temperature anomalies in mechanical behavior could be expected.

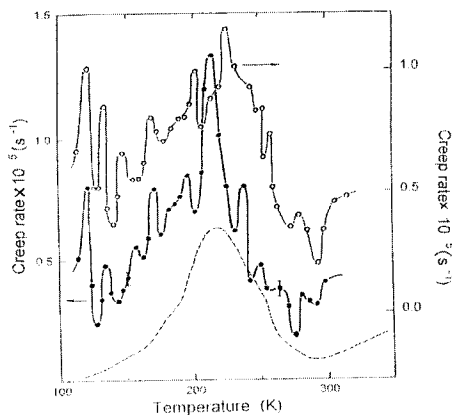


Fig. 1. Reproducibility of the creep rate spectra (compressive $\sigma = 20$ MPa, $t = 10$ s) for two samples of a model epoxy-amine DGEBA-DDM/60BAN network taken from two separate batches (Ref. 6). The dashed line corresponds to their dynamic mechanical spectrum contour of 1 Hz (Ref. 10).

Figures 2-4 really demonstrate such relations regarding the fracture stress σ_F vs. T dependences for various materials, viz. poly(vinyl butyral) (PVB), porcelain, poly(vinyl chloride) (PVC) and an epoxy network.

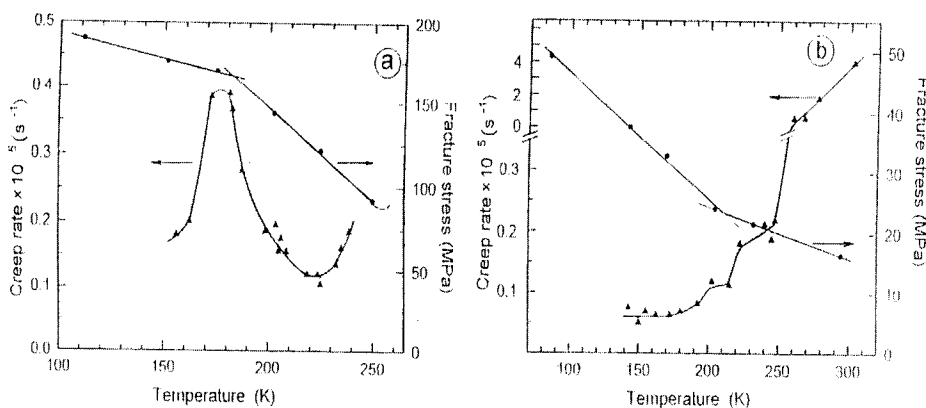


Fig. 2. (a) Temperature dependences of the low-temperature creep rate (\blacktriangle ; tensile $\sigma = 28$ MPa, $t = 30$ s) and of tensile fracture stress (\bullet) in poly(vinylbutyral); (b) Temperature dependences of microplasticity (\blacktriangle ; compressive $\sigma = 9$ MPa, $t = 10$ s) and of compressive fracture stress (\bullet) in unannealed porcelain.

One, two, or three bends in the σ_F vs. T plot are observed at low temperatures of sub- T_g relaxations; these bends may result in both increasing and lowering the slope of this

dependence with temperature. Thus, the only low-temperature creep rate peak, at ca. 180 K, in PVB corresponded to the onset of a much more intense drop in fracture stress with temperature (Fig. 2a), whereas the onset of microplasticity at 200-220 K in unannealed porcelain led, on the contrary, to a decrease in the slope of the σ_F vs. T plot, beginning just from these temperatures (Fig. 2b).

More complex creep rate spectra and, simultaneously, two or three bends in the σ_F vs. T dependences were obtained for PVC and an epoxy-amine network (Figs. 3 and 4). The following points should be noted here.

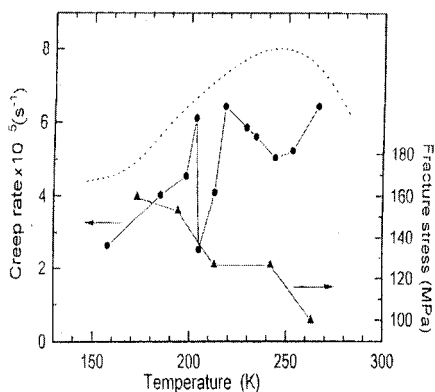


Fig. 3. Temperature dependences of the creep rate (●; compressive $\sigma = 23$ MPa, $t = 30$ s) and of tensile fracture stress (▲) in poly(vinyl chloride) for 30 s longevity under load. Dotted line is a contour of mechanical loss spectrum at 1 Hz.

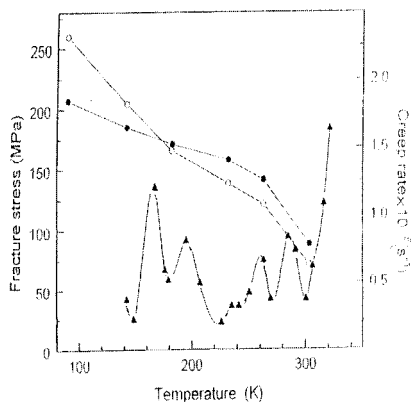


Fig. 4. Temperature dependences of the creep rate (▲; compressive $\sigma = 20$ MPa, $t = 30$ s) in epoxy-amine network D-450 in the region of sub- T_g relaxations and of the fracture stress (tension ● or torsion ○) for 30 s longevity under load.

For PVC, instead of a broad β -relaxation mechanical loss peak (1 Hz) with maximum at ca. 240 K, a pair of neighboring creep rate peaks, at ~ 200 and 220 K, and the onset of a new peak above 240 K are observed; owing to lower frequencies of measurements (10^{-3} - 10^{-2} Hz), this doublet may also be related to β -relaxation. The changes in the slope of the σ_F vs. T plot occurred at about the same temperatures. Consequently, the temperature anomalies in strength may be predicted more distinctly from the creep rate than from a mechanical loss spectrum. Such inference also followed from the same correlations found previously for PMMA (Ref. 3) and PS (Ref. 5).

The effect of bifurcation of the β -relaxation peak in the spectrum of PVC, with arising of the low-temperature satellite peak at 200 K, is similar to that observed at ca. 250 K and 300 K for PS (Ref. 5). It can be assumed that this was induced by the presence of two dominating

types of molecular packing in nanovolumes of a glassy polymer, reflecting its nanostructural heterogeneity. Interestingly, in both cases of PS (Ref. 5) and PVC (Fig. 3), the most sharp change in the slope of the σ_F vs. T plot began from the temperatures of satellite peaks, obviously, in 'unfreezing' of segmental motion at the sites with the most loosened segmental packing.

In the creep rate spectrum of epoxy network D-450, two pairs of neighboring peaks are present, at 165-190 and 260-285 K (Fig. 4). Again, the bends in the σ_F vs. T plots correlate rather with the lower-temperature constituents of these doublets. At 165 K, the strength only responded to the creep rate peak arising under torsion.

The observed nonmonotonies in the course of the σ_F vs. T dependences may be treated as a result of interaction of two physical processes which proceed in parallel in a loaded solid, deformation and fracture. On the one hand, deformation can sometimes create the prerequisites for enhancing the local over stresses, thus facilitating the fracture process. Large inelastic deformations (orientation) strengthen the polymer. Meantime, for brittle or quasi-brittle fracture of a solid, the possibilities of relaxation of local over stresses due to small localized deformations are of special significance. In kinetic models of brittle fracture (Refs. 11,13), the anomalies in temperature dependence of strength are analyzed proceeding from: (a) the ratio of over stress relaxation time, τ_R , to longevity under load, τ_F ; (b) the suggestion of proceeding of the fracture process at alternative, e.g., permanently diminishing local stresses, and (c) different contribution of local inelastic deformation to the fracture process at different temperatures.

Thus, suppression of local deformation below 180 K in PVB (Fig. 2a) obviously predetermines its brittle-ductile transition. In this case, when $\tau_R \gg \tau_F$, the fracture process occurs at increased or alternative local over stresses, and PVB breaks below 180 K, at lower mean stresses than predicted by extrapolation of the linear σ_F vs. T plot from higher temperatures. On the other hand, for porcelain (Fig. 2b) and epoxy network under torsion (Fig. 4), local deformation processes diminish the over stresses and provide higher strengths at 180-200 K than expected from extrapolation of the σ_F vs. T dependence from low temperatures.

Relaxation behavior of polymer binder in composites. It was intended to reveal the peculiarities of the relaxation behavior of polymer binder in composites by CRS. The largest effect could be expected for the composite with the finest filler particles providing the highest values of interfacial area and volume fraction of the binder located near the interfaces.

Figure 5 shows the changes in the spectrum of epoxy network caused by addition, in the ratio of 1:2, of mineral (diabase) particles of 10, 160 or 630 μm size. Indeed, the creep rate spectra of the filled epoxy networks underwent pronounced changes in the region of sub- T_g

relaxations, 150 - 300 K, which depended to some extent on diabase dispersity (Fig. 5).

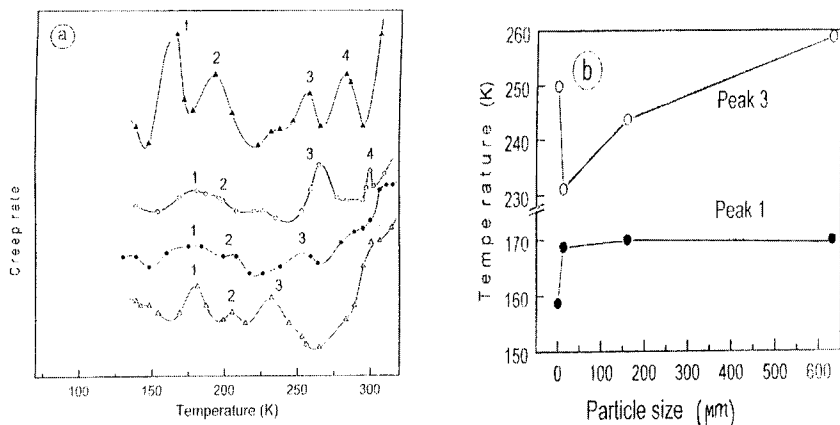


Fig. 5. (a) Creep rate spectra (compression, $t = 30$ s) for epoxy-amine network D-450 (\blacktriangle , $\sigma = 20$ MPa) and its composites with diabase (1:2) particles of various sizes (\circ 630 μm , \bullet 160 μm , Δ 10 μm , $\sigma = 30$ MPa); (b) Temperatures of creep rate peaks vs. particle size.

If peak 1 broadened, diminished and shifted by ca. 10 K to higher temperatures for all the composites studied, peaks 3 and 4, corresponding to segmental relaxations in the region of β -relaxation, diverged after adding the filler to epoxy network. Peak 4 became less pronounced and shifted by ca. 20 K to higher temperatures whereas peak 3 slightly increased, both in height and temperature, when using coarse diabase particles only. At the same time, its temperature decreased by 30 K for the composites with 10- μm particles.

Hence, the filler affected molecular mobility in two opposite ways. On the one hand, impeded mobility of segments located in the immediate vicinity of diabase surface evidently took place. On the other hand, displacement of peak 3 to lower temperatures may be interpreted as formation of sites with loosened segmental packing in a binder owing to entropy barriers caused by filler particles and to the polymer confinement effect.

Following the data shown in Figs. 4 and 5, the 'critical' temperatures of changes in mechanical behavior of composite may differ noticeably from those in the unfilled network binder; they may depend, presumably, on a type of filler, its dispersity, polymer/filler ratio, etc.

Nanoscale dynamic/compositional heterogeneity in complex polymer systems. Unlike glassy polymers with a rather narrow glass transition range, $\Delta T_g \approx 10\text{-}20$ K, complex miscible polymer systems may show an extraordinary broad $\Delta T_g \approx 50\text{-}100$ K; this was observed for blends, IPNs, and others (examples can be found in Refs. 14-16). The most probable reason

for such effect may be the dynamic heterogeneity of segmental dynamics in the glass transition due to compositional or physical inhomogeneity, at least on the nanoscopic scale. It must result in a dispersion of glass transitions, and the overall effect might be a single, very broad ΔT_g range. Meantime, the generally used relaxation spectrometry techniques have failed to subdivide a broad glass transition region for any constituents.

Recently, CRS was successfully used for detailed analysis of segmental relaxations and heterogeneity of segmental dynamics within and near the broad glass transition range for a series of IPNs based on poly(propylene oxide)-based polyurethane (PUR)/butyl methacrylate-triethylene glycol dimethacrylate copolymer (BMA copolymer) with regularly varied composition (Ref. 7). The BMA copolymer content ranged from 32 to 89 wt.-% in these materials.

Such traditional techniques as DSC or dielectric relaxation spectrometry were capable of demonstrating only a continuous region of glass transitions. Thus, one heat capacity step extending from 200-220 to 270-280 K was observed over the entire compositional range for these IPNs, and their T_g was around 250 K, irrespective of composition. In contrast, the creep rate spectra of these systems exhibited a complex structure, viz., up to 5 - 8 discrete or partly overlapping constituents as the peaks with maxima or contour nonmonotonies such as steps or shoulders upon the edge of a basic peak. The contours of IPN spectra turned out to be of a peculiar shape for each composition. This is illustrated by Fig. 6 where the creep rate spectra for three of the IPNs studied are presented. The insets with extended ordinate scales indicate the minute CR peaks.

Figure 6 shows that the main creep rate peak shifted upwards, from 280 K to 290 K and to 295 K, with an increasing BMA copolymer content in the IPNs but, in addition, the spectral contour as a whole cardinally changed with composition as well.

In this research (Ref. 7), CRS allowed not only to differentiate a number of constituent relaxations within and near the broad ΔT_g range but also made possible molecular assignments of the multiple creep rate peaks.

We proceeded from an assumption about two origins of dynamic heterogeneity around T_g :
 (a) the presence of nanodomains with various compositions in a miscible system and
 (b) possible substantial differences in segmental packing density within nanodomains of the same composition.

Besides, the CRS data analysis was based on the experimental evidence of common segmental nature of the α - and β -relaxation transitions in flexible chain polymers (Ref. 15). According to this conception, segmental dynamics in a polymer around T_g is determined by intermolecularly

cooperative (α -relaxation) and partly cooperative ('intermediate relaxations') or kinetically independent noncooperative segmental motions (β -relaxation). The main thrust herein is that the moving segment, controlling dynamics and conformational transformations in chains, virtually coincided in size with a Kuhn statistical segment, mostly of 1.5-3 nm length in flexible chain polymers, at all temperatures $T \geq T_\beta$.

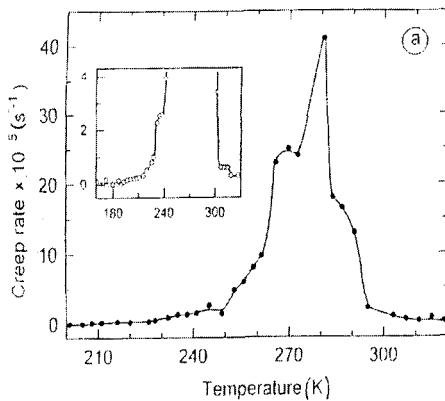
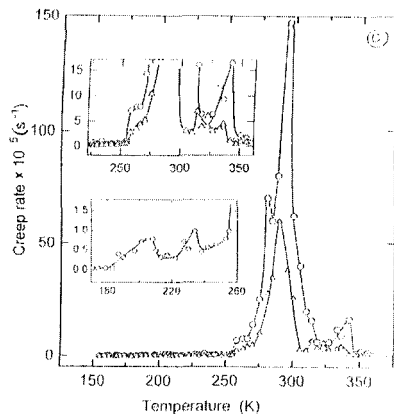
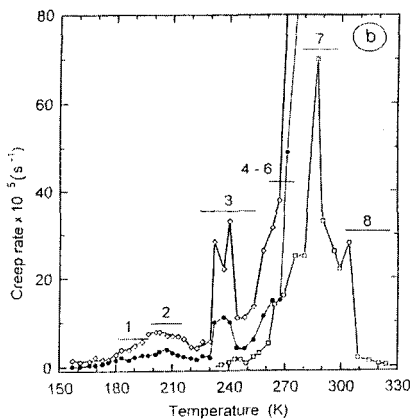


Fig. 6. Creep rate spectra measured under tension and indicated experimental conditions for the polyurethane/butyl methacrylate copolymer-based IPNs.

(a) 68PUR/32BMA, $\sigma = 0.3$ MPa, $t = 10$ s (\circ) or 30 s (\bullet);

(b) 39PUR/61BMA, $\sigma = 0.3$ MPa, $t = 30$ s (\square), $\sigma = 0.5$ MPa, $t = 10$ s (\diamond) or 30 s (\bullet) (Temperature ranges 1–8 correspond to the predicted temperatures of 'unfreezing' of different kinds of segmental motions within or close to extraordinarily broad IPN glass transition (Ref. 7).)

(c) 20PUR/80BMA, $\sigma = 0.3$ MPa, $t = 10$ s (\circ) or 30 s (Δ)



Then, the 'anomalies' of glass transition manifestation in complex polymer systems are treated as a partial or total collapse of intermolecular cooperativity of segmental motions, with a decrease in the parameter of cooperativity Z from typical values of 3-5 at low frequencies down to unity, because of loosening molecular packing or mixing with foreign molecules. Significantly, the regular relations between transition parameters and main molecular characteristics of polymers have been found experimentally (Ref. 15). Validity of this approach to interpretation and prediction of the peculiarities of glass transition has been

corroborated for plasticized polymers, block and graft copolymers (Ref. 15) and, recently, for miscible blends (Ref. 16).

We assumed that the IPNs studied also obeyed the above common conception; indeed, the creep rate spectra responded in a discrete manner to 'unfreezing' of different kinds of Kuhn segment motions over the temperature region around T_g .

As a matter of fact, in this case, up to eight kinds of such motions, cooperative and partly cooperative or non-cooperative, might be predicted in the PUR/BMA-copolymer-based IPNs studied; their expected characteristics, estimated by other techniques or calculated (Refs. 7,15), are given in Table 1. It is evident that motions 2, 6 and 7 are peculiar to the sites with segmentally mixed structure whereas the other, 1, 3, 4, 5 and 8, indicate phase separation, at least on the nanometer scale, in these 'single-phase' systems since they must be related to the neat constituent networks.

Our expectations (Table 1) compared with the creep rate spectra, given in Ref. 7 and, partly, in Fig. 6, allow to conclude that (a) the spectra cover just the same temperature range, from 170-180 to 320-340 K, as predicted, and (b) the creep rate peak temperatures satisfactorily coincide with the expected temperatures for the relevant motions.

Table 1. Possible kinds of segmental motions within (or close to) anomalously broadened glass transition in the PUR/BMA-copolymer-based IPNs, and expected approximate values of their parameters (Ref. 7)

No.	Segmental motion	T (K) at 10^{-2} Hz	Activation energy Q (kJ mol ⁻¹)	Intermolecular cooperativity parameter Z
1	Arrhenius β -relaxation in poly(propylene oxide) (PPO)-based PUR network	170 - 190	50 - 55	1
2	Arrhenius β -relaxation, when contacting PPO chains with PBMA chains	200 ± 10	55 - 60	1
3	Partly cooperative, 'intermediate' relaxations in PUR network	220 ± 10 250 ± 10	—	2 3
4	Cooperative α -transition in PUR network	270	220 - 250	4
5	Arrhenius β -relaxation in (a) linear PBMA (b) BMA copolymer network	270 270	80 - 90 80 - 100	1
6	Arrhenius β -relaxation, when contacting PBMA chains with PPO chains	260	70 - 80	1
7	Cooperative motion of PBMA and PPO (in PUR) neighboring segments	280 - 290	~200	3 - 4
8	Cooperative α -transition in (a) linear PBMA (b) BMA copolymer network	300 - 315 300 - 330	200 - 230	≈ 3

Each spectrum mostly included some of the peaks listed in Table 1, although the spectrum for the 39PUR/61BMA copolymer composition exhibited virtually their total set (Fig. 6b).

Finally, on this basis, an approach to a semiquantitative estimation of the nanoscale compositional heterogeneity and miscibility degree in these IPNs from CRS data was suggested (Ref. 7). This was attained by comparing the heights of spectral constituents associated with the neat networks or segmentally mixed nanodomains. The nanoscale compositional heterogeneity and incomplete compatibility of both constituent networks was demonstrated for all of these 'single-phase' IPN compositions.

CONCLUSION

The data obtained confirm that CRS is a sensitive technique for prediction of temperature anomalies in mechanical properties, for revealing the influence of a filler on relaxations in polymers, and for analysis of nanoscale dynamic/compositional heterogeneity in complex polymer systems.

ACKNOWLEDGEMENT

This work was supported by the Russian Fund for Basic Research (grant No. 97-03-32643) and INTAS (Project No. 97-1936)

REFERENCES

- (1) V.A. Bershtein, N.N. Peschanskaya, A.B. Sinani, V.A. Stepanov, *Fiz. Tverd. Tela* **22**, 767 (1980) [*Sov.Phys.Solid State* **22** 448 (1980)]
- (2) V.A. Bershtein, N.N. Peschanskaya, V.A. Stepanov, *Vysokomol. Soedin., Ser. A* **22**, 2246 (1980)
- (3) N.N. Peschanskaya, P.N. Yakushev, A.B. Sinani, V.A. Bershtein, *Thermochim. Acta* **238**, 429 (1994)
- (4) N.N. Peschanskaya, V.Yu. Surovova, P.N. Yakushev, *Fiz. Tverd. Tela* **37**, 2602 (1995)
- (5) N.N. Peschanskaya, P.N. Yakushev, A.B. Sinani, V.A. Bershtein, *Macromol. Symp.* **119**, 79 (1997)
- (6) V.A. Bershtein, N.N. Peschanskaya, J. Halary, L. Monnerie, *Polymer*, submitted
- (7) V.A. Bershtein, P.N. Yakushev, L. Karabanova, L. Sergeeva, P. Pissis, *J. Polym. Sci., Polym. Phys.* **37**, 429 (1999)
- (8) N.A. Zlatin, N.N. Peschanskaya, V.V. Shpeizman, *Zh. Tekh. Fiz.* **57**, 1438 (1987)
- (9) V.V. Shpeizman, N.N. Peschanskaya, B.I. Smirnov, Yu.P. Stepanov, *Fiz. Tverd. Tela* **31**, 101 (1989)
- (10) J.L. Halary, D. Bauchi re, R.L. Lee, L. Monnerie, *Polimery* **42**, 86 (1997)
- (11) V.A. Stepanov, N.N. Peschanskaya, V.V. Shpeizman, *Strength and Relaxation Phenomena in Solids* (in Russian), Nauka, Leningrad 1984
- (12) V.A. Stepanov, N.N. Peschanskaya, V.V. Shpeizman, G.A. Nikonov, *Int. J. Fracture* **11**, 851 (1975)
- (13) V.A. Stepanov, V.V. Shpeizman, *Mater. Sci. Eng.* **49**, 195 (1981)
- (14) J.J. Fay, C.J. Murphy, D.A. Tomas, L.H. Sperling, *ACS Symp. Ser.* **424**, 415 (1990)
- (15) V.A. Bershtein, V.M. Egorov, *Differential Scanning Calorimetry of Polymers. Physics, Chemistry, Analysis, Technology*, Ellis Horwood, New York 1994
- (16) V.A. Bershtein, L.M. Egorova, R.E. Prud'homme, *J. Macromol. Sci.-Phys.* **B36**, 513 (1997)